Nazarbayev University School of Medicine

Department of Biomedical Sciences

Master of Molecular Medicine

INVESTIGATING THE DEVELOPMENTAL POTENTIAL OF TRIPLE HP1 KNOCK-OUT ES CELLS

Author: Aslan Temirkhanov, MD

Supervisor: Professor Prim Singh, PhD

ORCID iD: 0009-0004-4323-2554

2025

Acknowledgements

I wish to express my gratitude to Professor Prim Singh for the exceptional opportunity to collaborate with his laboratory and team. This was a remarkable opportunity to enter the scientific realm, with specific gratitude for the provision and access to the essential equipment, reagents, and laboratory facilities.

I am profoundly appreciative of my amazing teammates and research assistants for their unwavering generosity and support along this trip. I extend my sincere gratitude to Yergali Bexeitov for his tremendous mentorship, which encompassed instruction in operational procedures, guidance in navigating the laboratory environment, and the impartation of essential practical skills and information important to my progress. His mentorship and assistance have been vital throughout our study endeavor.

CONTENTS

ABSTRACT

During the process of development, there is a limitation placed on the potential for development. The destiny of cells is flexible in the beginning stages of development; however, as the process of development continues, cells become more specialized, eventually giving rise to monopotential differentiated cells that populate adult tissues. Recent research has suggested that the cellular identity of differentiated cells is protected by an epigenetic mechanism that involves trimethylation of the ninth lysine on histone H3 (H3K9me3)-marked (hetero)chromatin. This mechanism is thought to be responsible for the safety of differentiated cells. Together with its binding partner HP1, H3K9me3 is responsible for the assembly of large heterochromatin-like domains in the euchromatic arms of chromosomes. There are three isoforms of Heterochromatin Protein 1 (HP1)which are able to bind to H3K9me3. These isoforms are HP1α, HP1β, and HP1γ. Here, we test the hypothesis that such domains regulate the identity and plasticity of the differentiated state. To that end, we will utilise our murine HP1TKO ES cells in which all three mammalian HP1 genes, encoding the HP1 isoforms HP1α, HP1β, and HP1γ are deleted. The purpose of this study is to investigate the impact that ablating HP1 function has on the capacity of HP1TKO embryonic stem cells to differentiate into mesodermal progenitors and then to keep their cellular identity after the differentiation process has been completed.

Keywords: HP1, Heterochromatin protein 1, Cellular identity, Epigenetic rejuvenation, H3K9me3.

INTRODUCTION.

Tightly packed, often transcriptionally dormant DNA is referred to as heterochromatin. To ensure proper genome function, heterochromatin is established during early developmental stages through regulated epigenetic processes that must be maintained across generations from mother to

daughter cells. The presence of specific epigenetic markers that are vital for its formation, maintenance, and regulation distinguishes heterochromatin. Heterochromatin Protein 1 (HP1), widely recognized as one of the most significant heterochromatin markers, identifies and binds to di- and tri-methylated lysine 9 in histone H3 (H3K9me2/3), thereby creating a restrictive chromatin environment.

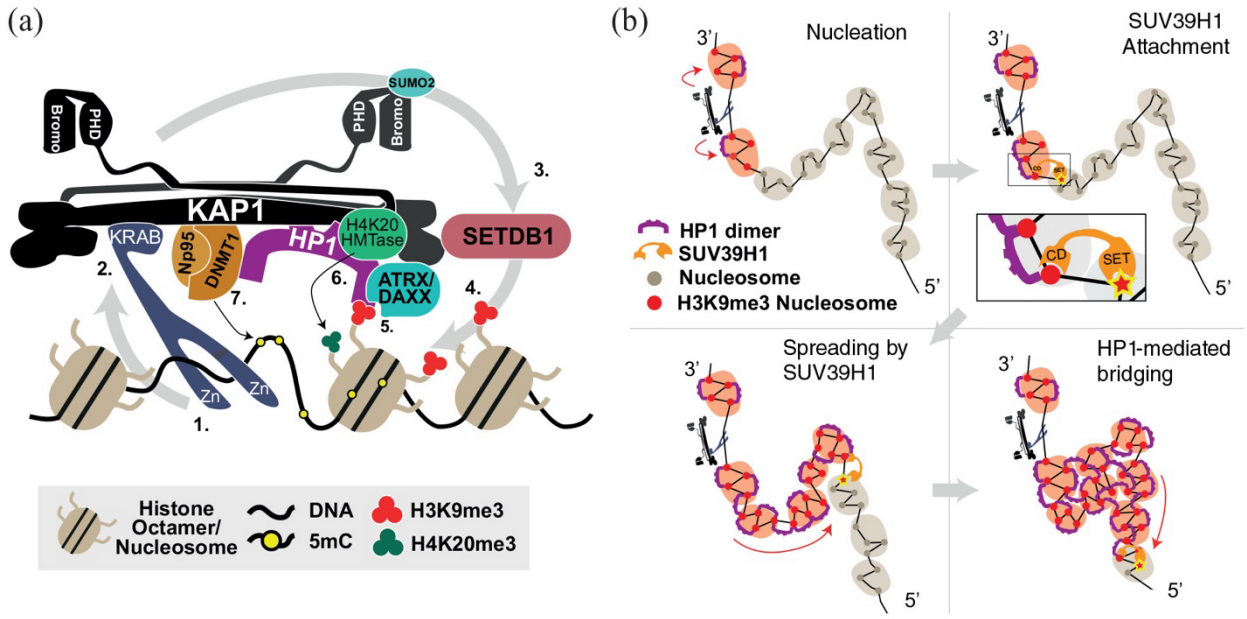

Figure 1: Microphase separation of heterochromatin-like domains/complexes at the KRAB-ZNF clusters on human chromosome 19 and their relation to the heterochromatic B4 sub-compartment Singh, P. B., & Newman, A. G. (2022, July 5).

H3K9me3 is a histone modification that has been found to be associated with cellular fate. Scientists remain uncertain about the mechanisms underlying cell reprogramming events, particularly during the early stages of embryonic development. Several papers were published discussing the function of H3K9me3 and its relationship with HP1. HP1 has the ability to identify and attach itself to H3K9me3, which assists in preserving the condensed or tightly packed structure

of DNA. Several papers have been published that discuss the topic of reprogramming and emphasize the significance of H3K9me3 and HP1 (would be good idea to put references here).

The microphase separation of HP1-mediated heterochromatin-like domains, especially at KRAB-ZNF gene clusters like those on human chromosome 19, is another crucial component of heterochromatin architecture. According to recent research, the assembly of these domains is started by tiny nucleation complexes that contain ATRX proteins and are about 1.5 kb in size. When KRAB-ZNF transcription factors attach to their DNA target sites via their zinc-finger motifs, this process starts. KAP1, which acts as a scaffold for the recruitment of other silencing factors, is subsequently recruited by the KRAB domain (Figure1a).

HP1 dimers reinforce the formation of a repressive chromatin environment by binding to KAP1 and concurrently identifying pre-existing H3K9me3 alterations through their chromodomain. Further deposition of H3K9me3 marks results from KAP1's SUMOylation, which improves its interaction with the histone methyltransferase SETDB1. The histone variation H3.3 is deposited concurrently by the ATRX-DAXX complex, which is linked to KAP1 and HP1, further solidifying the heterochromatin structure. In order to preserve cytosine methylation across cell divisions, this multiprotein complex not only forms a small zone of compact chromatin but also attracts enzymes like DNA methyltransferase 1 (DNMT1) (Figure 1a).

The histone methyltransferase SUV39H1 can create a positive feedback loop that allows the heterochromatin-like domain to grow after it has been nucleated. Existing H3K9me3 marks are recognized by SUV39H1 and extended along neighboring chromatin fibers; this process is maintained by HP1-mediated nucleosome bridging (Figure 1b). Larger, compartmentalized zones of heterochromatin known as the B4 sub-compartment are formed as a result of this spreading mechanism and are visible on Hi-C contact maps.

Models of microphase separation, which resemble block co-polymer behavior, provide a biophysical explanation for the development of these domains. A tiny positive Flory-Huggins interaction value ($\chi = 0.036$ per nucleosome) describes the slight incompatibilities in chromatin composition that promote the segregation of heterochromatin from euchromatin. HP1-mediated "clutches" of 2–10 H3K9me2/3-marked nucleosomes function as cooperative units rather than as individual nucleosomes, which is in line with observations of heterochromatin nanodomains (HNDs) in embryonic stem cells (reference).

Various HND classes have been distinguished based on the nucleation factors at play. For instance, there are differences in the size and chromosomal position of ATRX-, ADNP-, and PAX3/9-dependent HNDs. Specifically, the size distribution of ATRX-associated HNDs, which are present at LINE1 elements, is dictated by thermodynamic limitations of chromatin packing rather than just sequence. Heterochromatic domain compartmentalization in the nucleus is thought to be explained by early nucleation at KRAB-ZNF clusters, followed by spreading and HP1-mediated stability.

To understand the effects of HP1 depletion, one must comprehend the nucleation, dissemination, and stabilization of heterochromatin domains. Disruption of these mechanisms in HP1-TKO embryonic stem cells probably leads to improper chromatin segregation, which alters lineage determination and resulting in inadequate differentiation patterns during the development of embryoid bodies.

Different HP1 isoforms have different roles; HP1α is localised to silent heterochromatin, HP1β is vital for the maintenance of pluripotent cell lineages, while HP1γ functions in both silent heterochromatin and euchromatin thereby has the ability to regulates both active and inactive chromatin (Sales-Gil & Vagnarelli, 2020; Casale et al., 2021). Collectively, these isoforms ensure

resolution of DNA recombination intermediates and regulate non-essential transcription while facilitating ES cell differentiation.

Emerging data indicates that embryonic stem cells are distinguished by globally less compact chromatin structures and abnormally high chromatin protein dynamics, in addition to the unique localization of HP1 and H3K9me3. Compared to developed cells, ES cells have more open chromatin generally, with a higher proportion of euchromatin and less dense heterochromatin foci. The quantity of condensed, transcriptionally silent heterochromatin rises dramatically with differentiation (Meshorer & Misteli, 2006).

Furthermore, in ES cells, heterochromatin proteins like HP1 and core chromatin elements like histones show abnormally high mobility. This "hyperdynamic" chromatin environment offers the flexibility needed for upcoming lineage commitments and for quick transcriptional modifications. These proteins become more firmly attached to chromatin when cells differentiate, which also causes the chromatin landscape to become more rigid and transcriptionally limited (Meshorer & Misteli, 2006).

Furthermore, ES cells exhibit a high number of active histone modifications, including trimethylation at H3K4 and increased acetylation of histones H3 and H4. Repressive epigenetic markers, such as H3K9me3 and H4K20me3, are significantly increased upon differentiation, indicating the shift toward more stable gene silence and lineage-specific chromatin architecture (Meshorer & Misteli, 2006).

This change is also accompanied by modifications in DNA methylation patterns. DNA methylation levels in ES cells are lower at first and rise as differentiation progresses, supporting the suppression of genes inappropriate for the lineage and helping to stabilize the differentiated state (Meshorer & Misteli, 2006).

The research published in the journal Nature Cell Biology (reference?) examines the role of H3K9me3-dependent heterochromatin reprogramming during mammalian embryonic development with regard to alterations in cellular fate following fertilization. Mammals acquire epigenetic modifications from both parental contributions starting from fertilized eggs. These epigenetic alterations undergo substantial reprogramming to achieve embryonic totipotency post-fertilization. Short hairpin RNA (shRNA)-mediated depletion of the constitutive heterochromatin marker H3K9me3 results in rapid remodeling, as H3K9me3-regulated heterochromatin maintains or represses embryonic genes and inactivates the imprinted X chromosome throughout development. The absence of trimethylation and euchromatic histone-lysine N-methyltransferase (ehmt), which are responsible for the establishment or removal of the H3K9me3 mark in this experimental context, leads to the deregulation of genes, ultimately resulting in embryonic demise. Imaging resolution limitations and the lack of a regulatory environment have restricted the effective mapping of immunofluorescence labeling of H3K9me3 in vivo. Consequently, conducting genome-wide analyses of H3K9me3-dependent heterochromatin during preimplantation embryonic development is of paramount importance.

Recent research has defined the function of H3K9me3-marked heterochromatin in the early stages of development (reference?). In particular, cells show significant amounts of compacted, H3K9me3-marked heterochromatin over protein-coding genes during the development of the final endoderm. This is correlated with transcriptional suppression to preserve lineage fidelity (Nicetto et al., 2019). Genes unsuitable for the cell's future identity are kept silenced by this compressed chromatin state.

This compact heterochromatin experiences a significant decrease and rearrangement upon lineage commitment, such as differentiation into hepatic or pancreatic lineages. The activation of lineage-

specific genes necessary for the development of specialized tissues coincides with the decrease in H3K9me3 levels (Nicetto et al., 2019).

Importantly, loss of heterochromatin structure, premature or inappropriate gene expression, and improper lineage commitment are caused by genetic disruption of the enzymes involved in H3K9 trimethylation, such as SETDB1, SUV39H1, and SUV39H2. These cells frequently do not fully adopt the correct cellular identity, even though some differentiation markers, like albumin, may still be detectable. This underscores the critical role that H3K9me3-mediated heterochromatin plays in stabilizing developmental programs and suppressing lineage-inappropriate transcription during differentiation (Nicetto et al., 2019).

Future research should persist in examining the role of HP1 complexes in sustaining gene silencing and chromatin integrity throughout development. In the second paper "H3K9me3-heterochromatin loss at protein-coding genes enables developmental lineage specification" (Science) researchers also discuss the role of H3K9me3 saying that it suppresses recombination and gene expression at highly repeated DNA sequences. To extract and map compacted heterochromatin from samples with few cells, they devised an antibody-independent method. They found that early, undifferentiated cells at the germ-layer stage have high levels of densely packed heterochromatin, specifically decorated with H3K9me3, at protein-coding genes. This compacted heterochromatin undergoes significant rearrangements and reduction as the cells differentiate, along with the expression of genes specific to each cell type.

The data reveal that HP1 is critical for carrying out the proper chromatin organization and gene expression programs associated with ES cell identity and lineage specification (whose data?). The elimination of three isoforms of HP1 proteins in ES cells shows how this protein plays a delicate bipolar role for cell differentiation between stem cell maintenance and lineage decisions.

Lack of HP1 in cells causes relaxation of chromatin structure that results in high genomic plasticity, non-finished differentiation, and varied gene expression levels. These results reveal fundamental roles of chromatin regulators including HP1 in retaining the cell state/identity and suggest possible therapeutic uses in regenerative medicine and gene therapy.

HYPOTHESIS

When compared to wild-type ES cells, triple HP1 knock-out (HP1-TKO) mouse embryonic stem (ES) cells show altered differentiation potential. This can show up as variations in lineage specification.

AIMS

To investigate the developmental potential of triple HP1 knock-out mouse ES cells by comparing their differentiation into germ layers to wild-type cells using embryoid body (EB) formation and immunofluorescence staining with lineage-specific antibodies.

OBJECTIVES

- Cultivate a sufficient quantity of two cell lines: wild-type (WT) and triple knockout (TKO) mouse ES cells

- Generate embryoid bodies (EBs) from both WT and TKO mouse ES cells employing two random differentiation methods.

- Conduct immunofluorescence labeling for essential markers of pluripotency and germ layers (OCT4, TBXT, SOX17, PAX6).

- Obtain confocal images and assess marker expression patterns, intensity, and spatial distribution.

- Analyze WT and TKO EBs to discern any discrepancies in differentiating behavior.

- Analyze results within the framework of HP1's established functions in chromatin architecture and developmental control.

MATERIALS AND METHODS

Mouse embryonic stem cells (mESCs), including wild-type (WT) and triple HP1 knock-out (TKO, also referred to as the 10-5 line) cell lines, were used in this study. WT and TKO cell lines were cultured in T25 flasks during the first month to obtain sufficient cell numbers for embryoid body (EB) formation. Cells were passaged every two days at a dilution ratio of 1:8 or 1:16, depending on growth rate and confluency. All cultures were maintained at 37°C in a humidified incubator with 5% CO_2.

To maintain pluripotency and suppress spontaneous differentiation, the culture medium was supplemented with 2 µL of human leukemia inhibitory factor (LIF), 40 µL of CHIR99021, and 4 µL of PD0325901. LIF supports self-renewal through the JAK/STAT3 pathway. CHIR99021, a GSK-3 inhibitor, promotes Wnt/β-catenin signaling, and PD0325901, a selective MEK inhibitor, suppresses MAPK/ERK signaling. This combination—commonly known as the "2i system"—helps stabilize the naïve pluripotent state of mESCs.

Two different sources of CHIR99021 (Cell Signalling Technology, Inc – 54290S and Amadis Chemical – A25048) and PD0325901 (Cell Signalling Technology, Inc - 79241S and Amadis Chemical – A6561) were evaluated. Cells cultured with each source were seeded into 24-well plates at densities of 1000, 2000, and 4000 cells per well (values to be inserted) to compare potential differences in proliferation and morphology. After incubation, cell number and behavior were assessed microscopically.

Embryoid Body Formation

EBs were generated using two methods: the hanging drop technique and the spontaneous aggregation method. In the hanging drop method, droplets (20–25 µL) containing 1000, 2000 or 4000 cells were placed on the inner surface of petri dish lids and inverted over dishes filled with 15 mL of PBS and 2 mL of 0.1% gelatin to maintain humidity. LIF-free medium was used to promote spontaneous differentiation. Cell viability was assessed before droplet formation using trypan blue staining and hemocytometer counts.

For the spontaneous aggregation method, cells were seeded at $5x10^5$ and $1x10^6$ cells per dish directly into 10 mL LIF-free medium in bacteriological-grade petri dishes. This led to the random formation of EBs with more fused and irregular morphologies compared to the hanging drop approach.

EBs were monitored regularly by bright-field microscopy, and images were taken to document morphological changes. In EBs derived from WT cells, spontaneous contraction resembling beating cardiomyocytes was observed on days 9-10, indicating successful differentiation.

Immunofluorescence Staining

On day 14, EBs were collected for immunofluorescence staining to evaluate differentiation into the three germ layers. Fixation was performed using 4% paraformaldehyde (PFA) for 20 minutes at room temperature. Two permeabilization and blocking protocols were tested:

- **Protocol A**: Permeabilization with 0.5% Triton X-100 (2 min), followed by blocking in 2% BSA in PBS (1 h).
- **Protocol B**: Simultaneous permeabilization and blocking in PBS containing 0.2% Triton X-100 and 4% goat or donkey serum (30 min).

Each protocol was tested using WT and TKO EBs in four separate Eppendorf tubes. Following blocking, EBs were washed three times with PBS containing 0.1% Tween-20 (PBST), 15 minutes per wash. Primary antibodies were diluted 1:200 in 2% BSA and incubated overnight at 4°C.

The following **primary antibodies** were used:

Antibody	Marker	Targeted Germ Layer	Host Species
TBXT (Brachyury)	Mesoderm	Mesoderm	Goat
SOX17	Endoderm	Endoderm	Rabbit
PAX6	Ectoderm	Ectoderm	Sheep
OCT4	Pluripotency marker	Pluripotency	Rabbit

After washing, **secondary antibodies** and DAPI were added for 4 hours at room temperature in the dark:

- **Donkey anti-Sheep IgG (H+L), Alexa Fluor™ 488, Cross-Adsorbed** (Invitrogen, A11015) – used to detect **PAX6**, observed in the green channel (FITC filter)
- **Donkey anti-Goat IgG (H+L), Alexa Fluor™ 488, Cross-Adsorbed** (Invitrogen, A11055) – used to detect **TBXT**, also visualized in the green channel (FITC filter)
- **Donkey anti-Rabbit IgG (H+L), Alexa Fluor™ Plus 647, Highly Cross-Adsorbed** (Invitrogen, A32795) – used to detect **OCT4** and **SOX17**, observed in the far-red channel (Cy5 filter)

Blocking serum (goat or donkey) was matched to the host species of the secondary antibody to prevent nonspecific binding.

Staining quality was first evaluated using an EVOS fluorescence microscope. After confirming successful staining, the optimized Protocol B was used for the final experiment. Four tubes were prepared:

- Two tubes (WT and TKO) for TBXT + SOX17
- Two tubes (WT and TKO) for PAX6 + OCT4

Stained EBs were mounted onto 8-well chamber slides and imaged using a confocal microscope to assess differentiation status based on fluorescence signal intensity and localization.

RESULTS

1. Mouse ES cells colony morphology upon thawing and passage

Upon gathering results and observing under the microscope, it became evident that WT and triple HP1 knock-out (10-5) mESC lines adhered well and displayed colony-like features characteristic of pluripotent stem cells after freezing and two days of passaging. The overall colony distribution was discernible at 5x magnification, with the WT cells forming more distinct and densely packed colonies than the 10-5 cells. The 10-5 cells looked more scattered and loosely organized at 20x magnification, but the WT colonies displayed distinct boundaries and consistent cell shape. The TKO line showed certain abnormalities in colony boundaries and cell morphology.

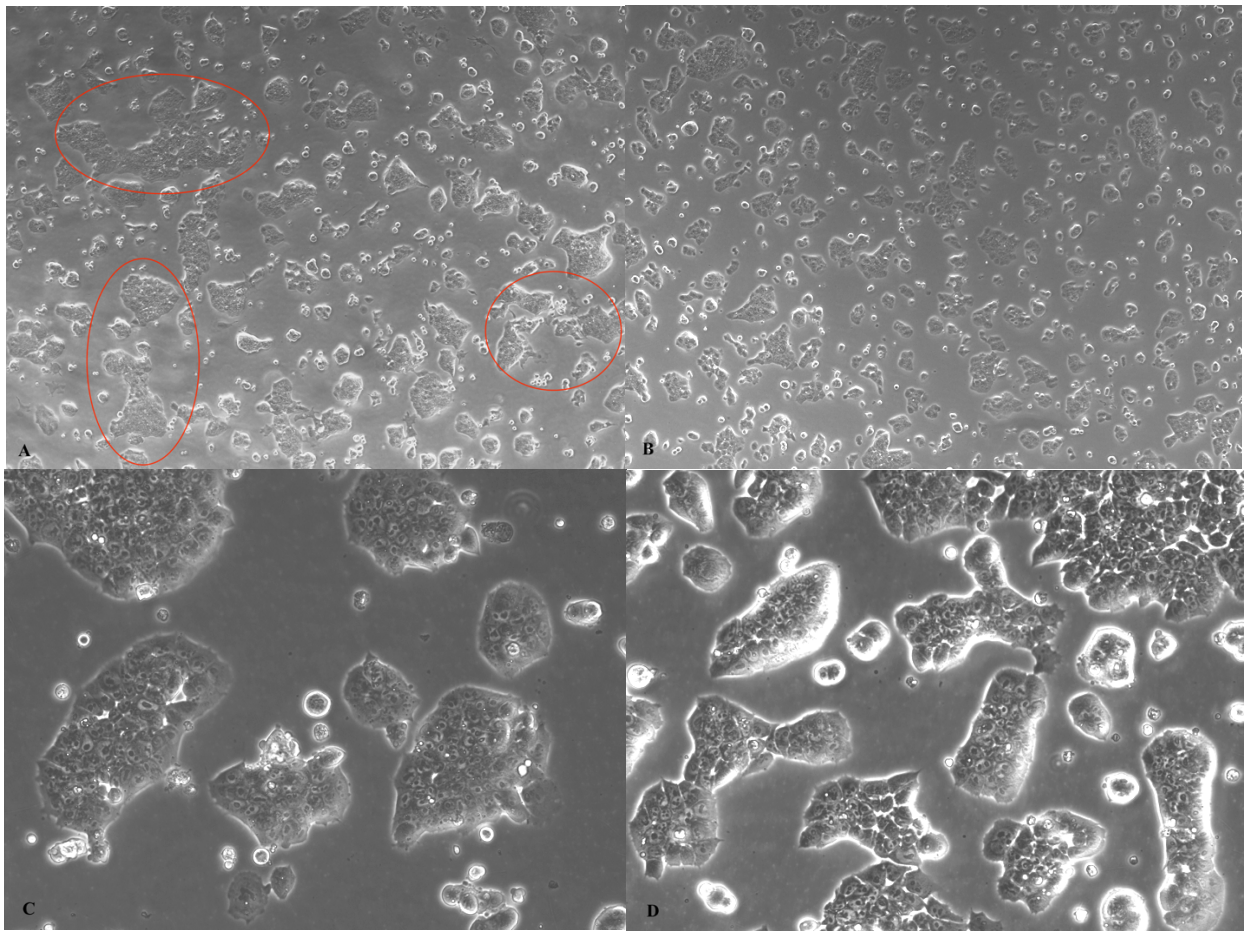

Figure 1. WT cells magnified 5 times (A); 10-5 cells magnified 5 times (B); WT cells magnified 20 times (C); and 10-5 cells magnified 20 times (D). I can hardly see the letters in the panels.

2. Early detection of structural variations in colonies.

Even though both lines adhered and multiplied, the spatial arrangement of the cells immediately showed variations. Clusters of WT cells tended to be denser and more cohesive.10-5 cells exhibited looser cell connections and a greater variety of forms. This could indicate that HP1 deletion has early consequences on chromatin control, impacting cell-cell adhesion or proliferation.

3. The Formation and Morphology of the Embryoid Body (EB)

Using spontaneous differentiation methods, it was possible to successfully produce embryoid bodies (EBs) from both wild-type (WT) and HP1 triple knockout (TKO, 10-5) mouse

embryonic stem cells. EB data are presented without method-specific attribution because the hanging drop and spontaneous aggregation procedures share appearances and overlap in culture timeframes. The two cell lines' reported morphological variations and developmental stages are the main points of interest.

3.1. Early Time Points of EB Morphology (48 hours)

Small, spherical EBs started to develop in both WT and TKO cultures 48 hours after seeding. Nonetheless, there were evident variations in the lines' compactness and organization.

With somewhat consistent morphologies across seeding densities (1000, 2000, and 4000 cells/drop or well), WT EBs tended to look more spherical, compact, and dense.

TKO EBs displayed looser cell packing and more asymmetrical outlines. Some EBs started to fuse at greater seeding densities (e.g., 4000), resulting in bigger, less distinct aggregates.

In contrast to TKO EBs, which have uneven shape and less structural cohesiveness, WT EBs seem more compact and symmetrical.

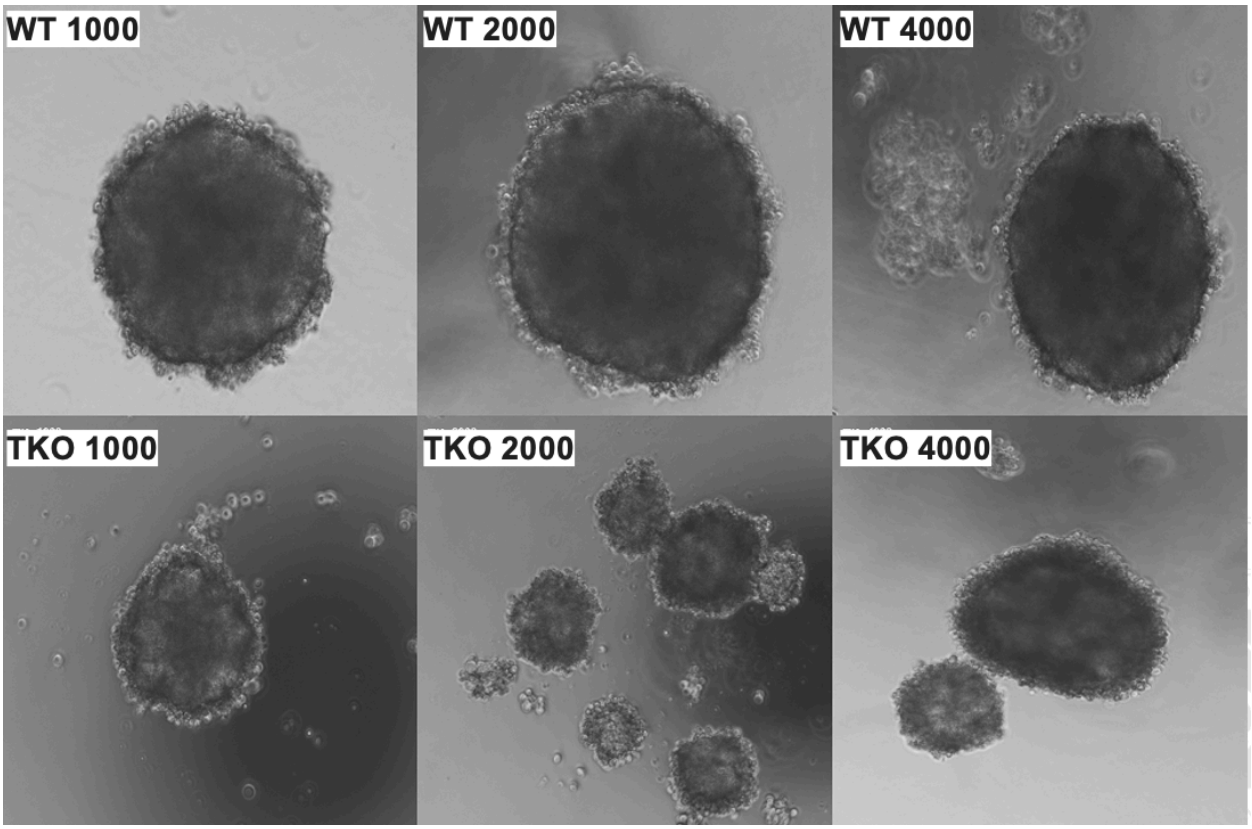

Figure 2. 48-hour representative pictures of EBs from WT and 10-5 cells (1000, 2000 and 4000 cells per EB).

3.2. Day 6 EB Development

Both wild-type (WT) and triple-knockout (TKO) cell lines' embryoid bodies (EBs) grew in size by day six of incubation. Some of them had diameters greater than 250–300 μm. The following patterns were noted:

- WT EBs typically retained a dense internal cell architecture and a well-defined, spherical form. On the other hand, bigger EBs occasionally showed peripheral abnormalities (for example, at 4000-cell seeding), which might be early indicators of edge instability or structural strain.
- The morphology of TKO EBs varied greatly, especially those implanted at 2000–4000 cells per drop. Some showed fractured appearance, uneven boundaries, or partial fusion, indicating irregular growth and aggregation.

According to these findings, the TKO cells exhibit decreased structural integrity and homogeneity by day 6, even if both lines are able to generate EBs.

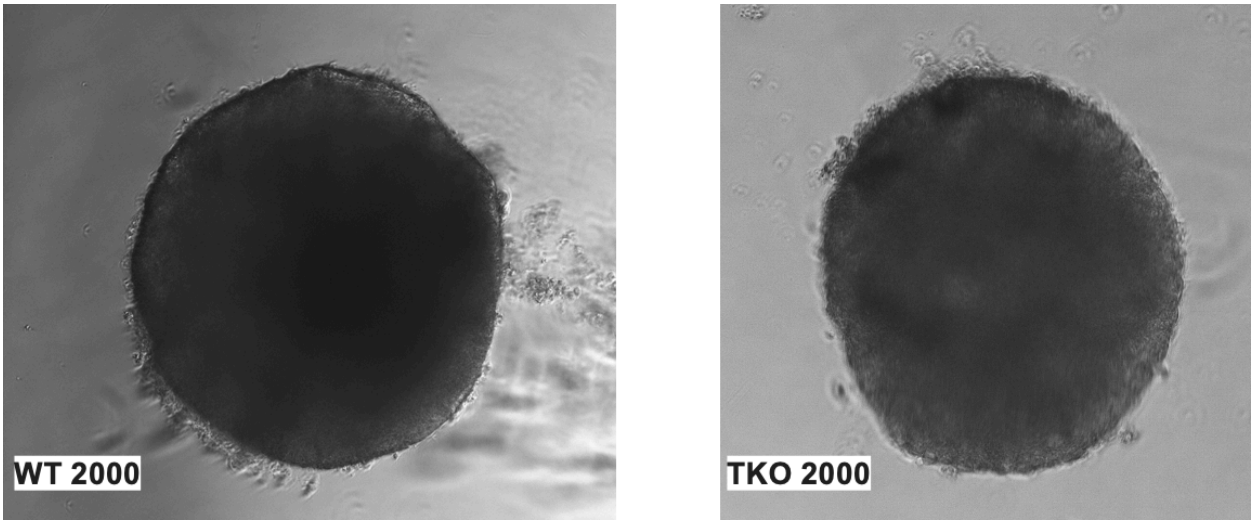

Figure 3. Day 6 representative EBs from both lines.

- WT, 2000 cells per drop — mostly circular, with compact borders; slight irregularities at the edges are apparent.

- TKO, 2000 cells per drop — more erratic in size and form, exhibiting indications of fragmentation or irregular development.

3.3. Cardiac-like Beating and Contractile Activity (Day 9)

By day 9, a subgroup of WT-derived EBs showed microscopic spontaneous contractile activity resembling cardiomyocyte beating. These regular contractions seemed to be associated with homogenous, spheroid morphology and were especially noticeable in larger EBs. At the same time point, no discernible comparable activity was found in EBs produced from TKO cells.

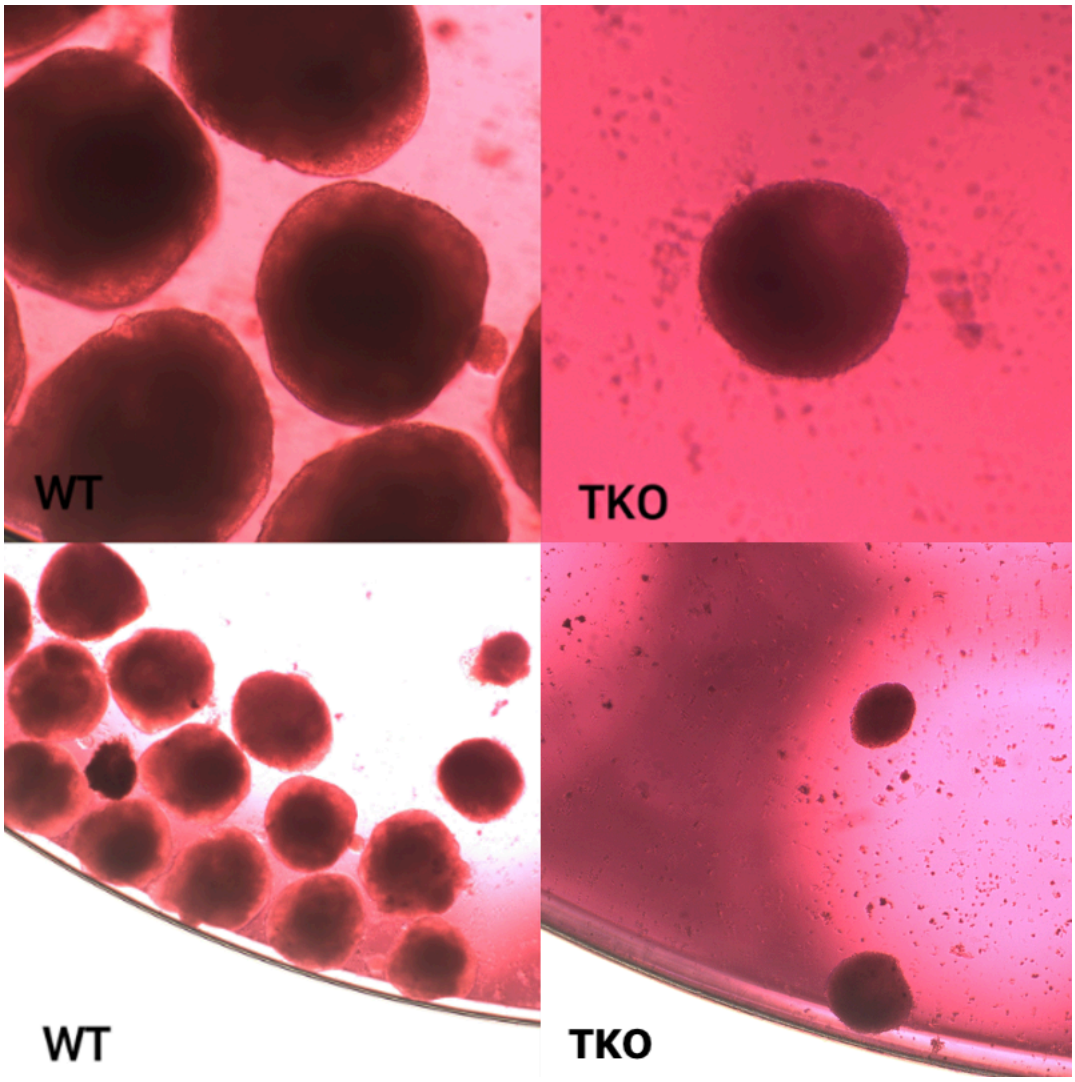

Figure 4. Compact, rounded shape of EBs on day 9.

High-density TKO EBs for comparison; WT EBs with discernible beating regions (not shown in the still image).

WT EBs regularly showed beating activity, but TKO-derived bodies did not.

3.4. Comparison of Seeding Densities

In order to maximize EB development, several seeding densities (1000, 2000, and 4000 cells) were used. Particularly in WT cells, intermediate densities (2000 cells) typically produced

the optimum balance between size, compactness, and single-EB formation. In contrast, even at low concentrations, TKO cells frequently created smaller or joined structures.

4. Immunofluorescence Staining of Embryoid Bodies

Embroid bodies (EBs) were produced from wild-type (WT) and triple HP1 knockout (HP1-TKO) mouse embryonic stem cells (mESCs), then exposed to immunofluorescence labeling on days 10–15. Key lineage and pluripotency markers— OCT4 (pluripotency), TBXT (mesoderm), SOX17 (endoderm), and PAX6 (neuroctoderm)—were visualised using confocal microscopy. Two separate staining sets—one for TBXT and SOX17 and one for OCT4 and PAX6—were employed to avoid antibody cross-reactivity. Nuclei were counterstained with DAPI.

- **TKO:**

SOX17 and TBXT (Fig.5-6):

- Along the outside of the EBs, TBXT expression (red) was seen often producing a peripheral dispersion. Individual EBs' TBXT intensity and dispersion differed.
- Though signal strength was not consistent across samples, SOX17 expression (green) seemed to be found in distinct clusters, usually in interior regions.
- TBXT and SOX17 co-localized only in limited extent; these markers usually occupied different domains.

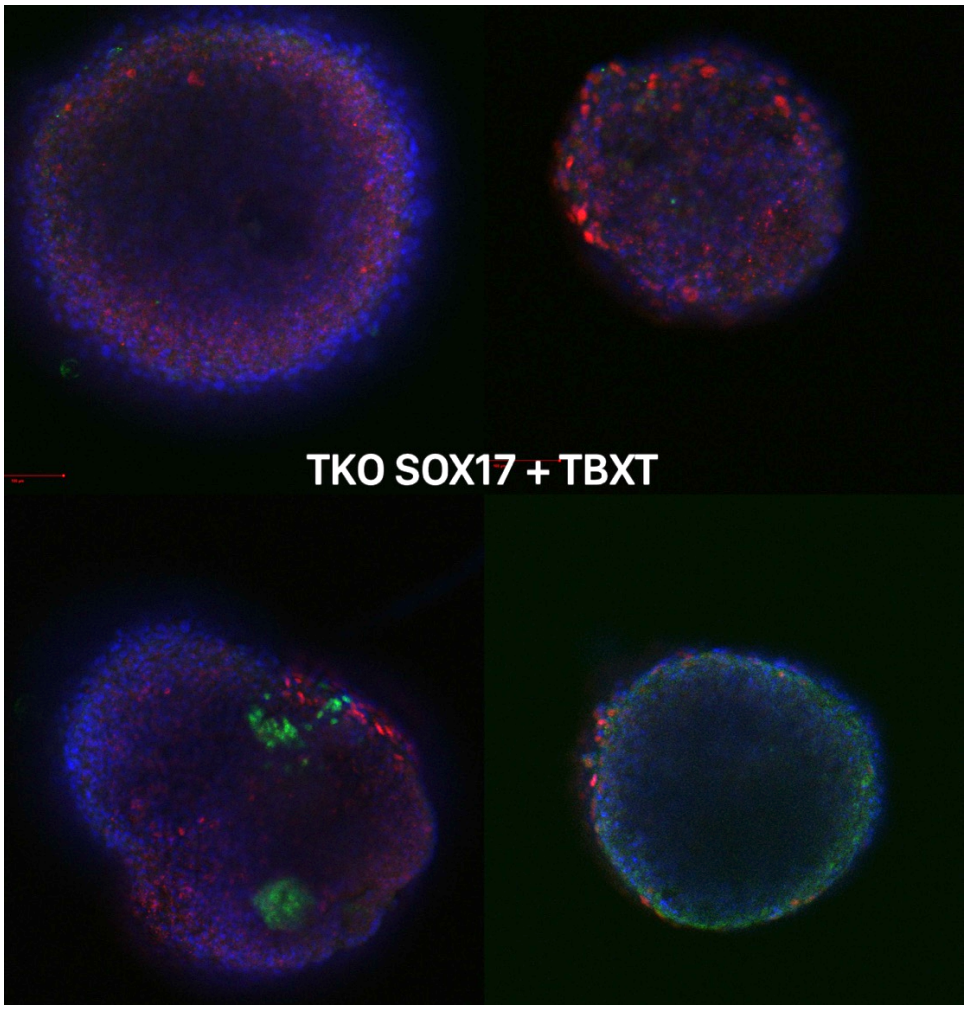

Figure 5. Immunofluorescence staining of TKO EBs for SOX17 and TBXT

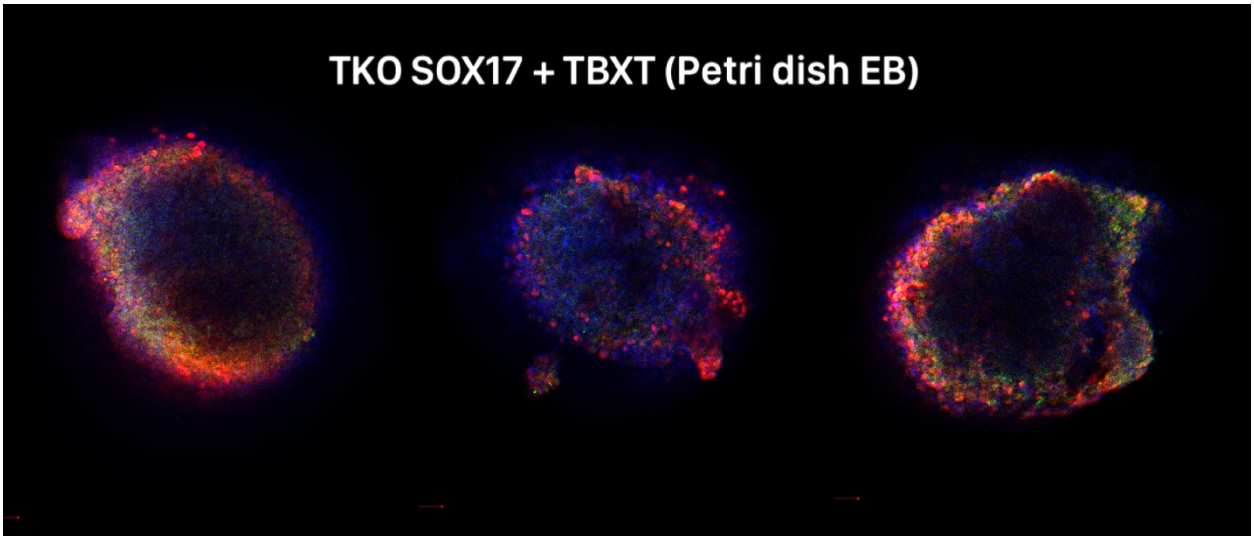

Figure 6. Immunofluorescence staining of TKO EBs for SOX17 and TBXT

PAX6 and OCT4 (Fig.7):

- While signal intensity varied, the OCT4 (red) signal was more detectable across EBs than PAX6 (green).
- In certain EBs, PAX6 was poor or even nonexistent, and it was frequently restricted to a small number of foci.
- Most of the time, the center areas of EBs had nearly no fluorescent signal, whereas the outer borders revealed clearer and more strong signals, particularly for both markers.
- Sometimes, OCT4 and PAX6 signals could be seen close but not significantly overlapping.

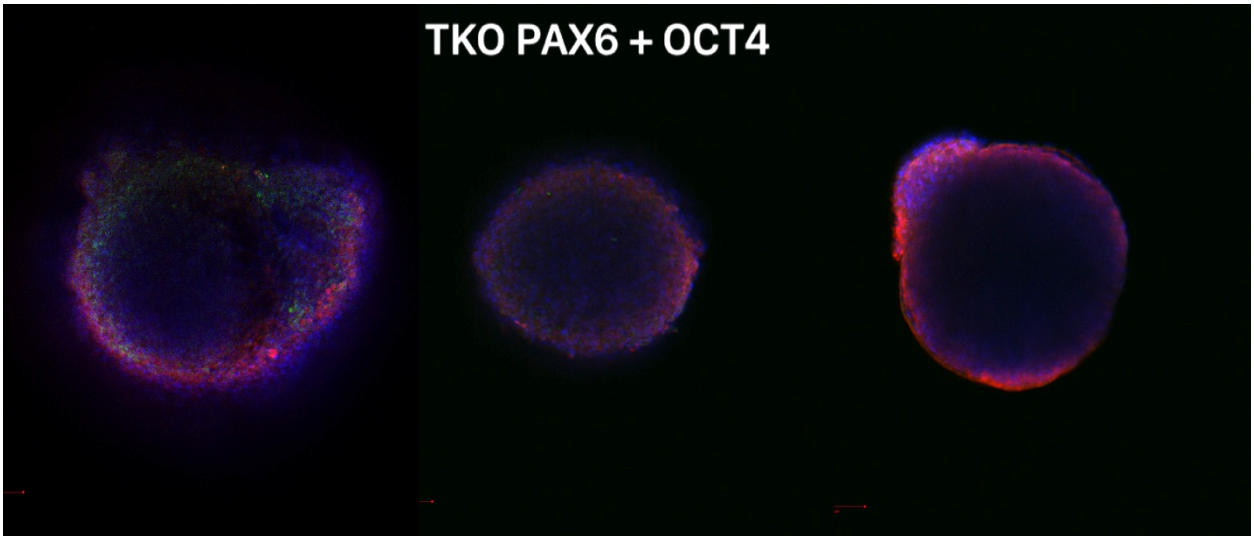

Figure 7. Immunofluorescence staining of TKO EBs for PAX6 and OCT4

- **WT:**

SOX17 and TBXT (Fig.8-10):

- At the edges of the EBs, TBXT (red) was dispersed uniformly or in a ring.
- Different internal regions showed SOX17 (green) staining. Although it varied significantly between samples, there was a noticeable spatial distinction between TBXT and SOX17.

- While some EBs displayed more pronounced expression than others, the signal strength was generally similar to EB from mTKO ES cells.
- The presence of internal circular formations in some EBs may represent developing cavities or partial aggregates (Fig.10). These observations may reflect both biological distribution and limitations in antibody penetration or imaging depth.

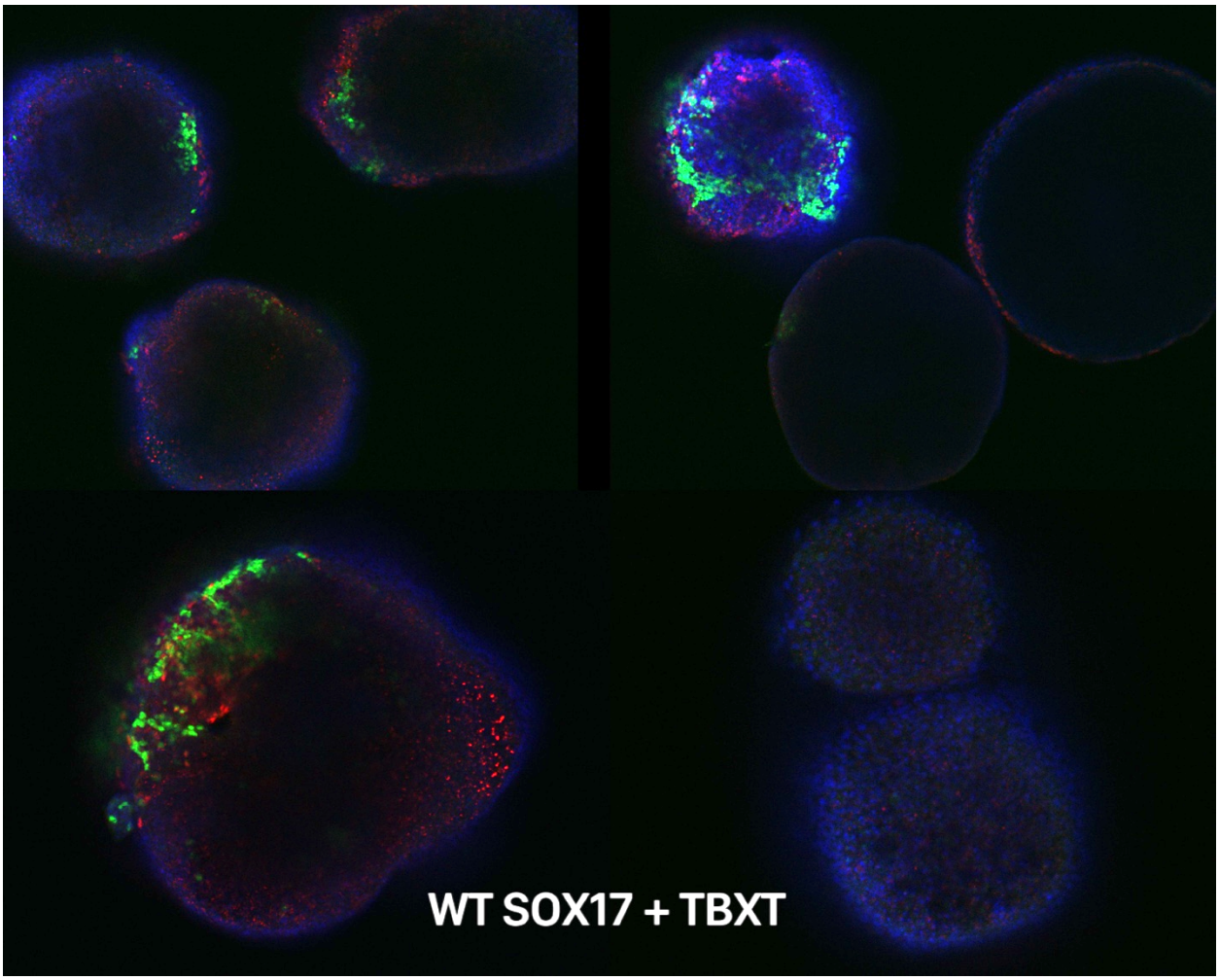

Figure 8. Immunofluorescence staining of WT EBs for SOX17 and TBXT

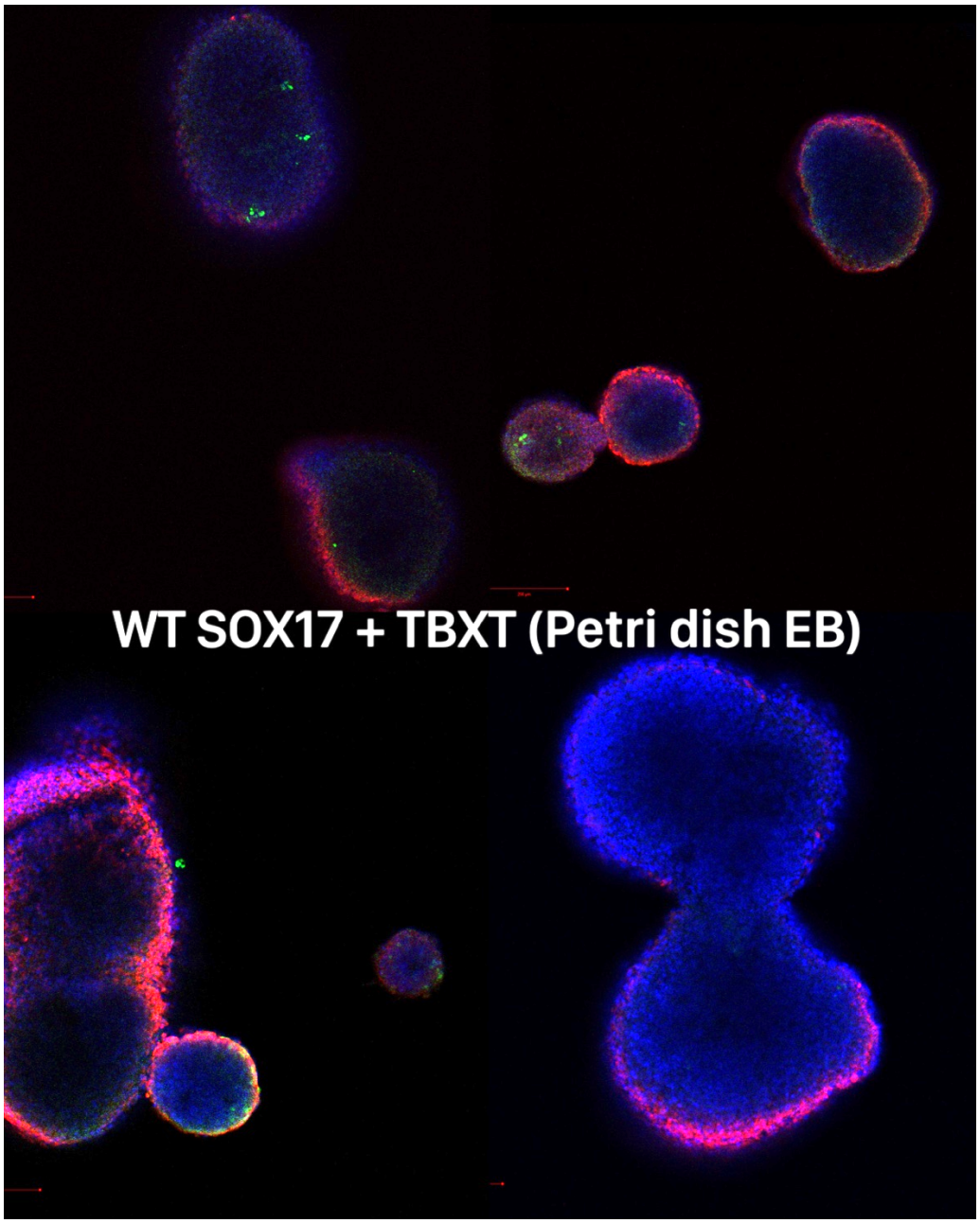

Figure 9. Immunofluorescence staining of WT EBs for SOX17 and TBXT

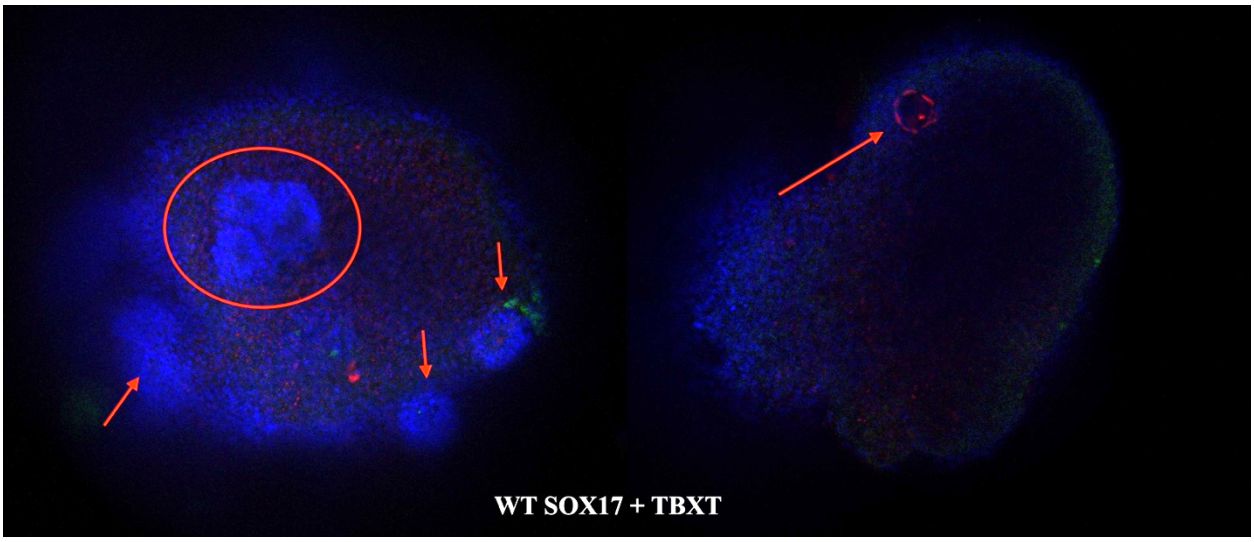

Figure 10. Immunofluorescence staining of WT EBs for SOX17 and TBXT

WHAT DO THE CIRCLES AND ARROWS MEAN?

PAX6 and OCT4 (Fig.11):

- Although the degree of OCT4 (red) expression varied from sample to sample, it was consistently present in all EBs.
- Several EBs had focal clusters of PAX6 (green), although the expression patterns varied among repetitions.
- OCT4 and PAX6 typically showed up in different areas, with little to no spatial overlap between the two markers.

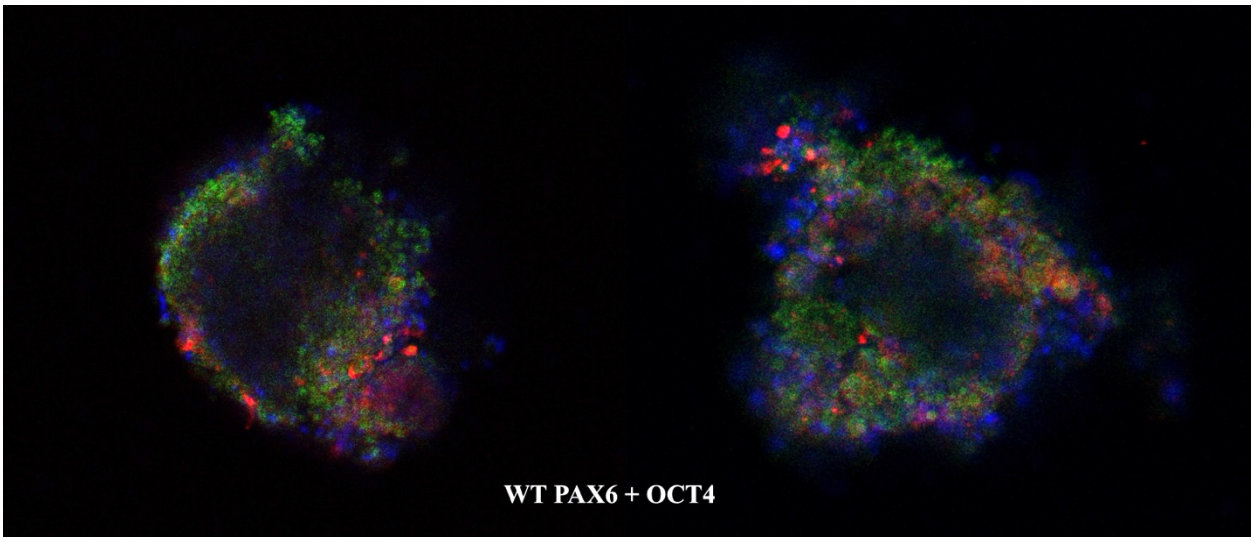

Figure 11. Immunofluorescence staining of WT EBs for PAX6 and OCT4

The PAX6 signal was consistently greater and more noticeable in WT EBs than in TKO EBs, where it was often weak or nonexistent, even though both groups had variation in expression patterns between individual EBs.

DISCUSSION.

Overall, triple HP1 knock-out (TKO) embryonic stem cells were able to form embryoid bodies (EBs), proving that the absence of HP1 proteins does not totally prevent ES cells from aggregating and starting early differentiation. Unfortunately, TKO EBs were more fragile and tended to be smaller than wild-type (WT) controls. The decreased quantity of undamaged TKO EBs at subsequent time periods, especially after pipetting and transfer procedures, was probably caused by this sensitivity, indicating a mechanical fragility.

One noteworthy finding was that TKO EBs at day 9 lacked the characteristic cardiac-like beating activity that is frequently observed in WT EBs. In the TKO condition, this could suggest delayed progression into contractile cell types like cardiomyocytes or defective mesodermal

differentiation. To elucidate this, additional research employing cardiac-specific markers would be necessary.

Emerging trends were identified by immunofluorescence staining; however, these results are preliminary due to the small number of stained EBs and sample variability. The EBs' periphery showed the greatest signal under both WT and TKO conditions, while the middle areas showed either no signal at all or a faint signal. This is probably caused by technical imaging restrictions rather than the lack of markers. Particularly in three-dimensional structures like EBs, confocal imaging has limited depth penetration, and fluorescence signals may weaken in deeper tissue layers.

Future research could investigate how the usage of EB sectioning can enhance interior visibility. In order to improve antibody penetration and facilitate in-depth examination of interior EB structures, methods like cryosectioning or microtome slicing should be taken into consideration because of weak or nonexistent core staining.

The emergence of small, circular structures inside a few WT EBs was one particularly intriguing discovery. These could be partial secondary aggregation, apoptotic bodies, or early cavity formation. Although their biological importance is still unknown, they should be studied further because they may affect the uniformity of staining or the penetration of antibodies.

Even though primary and secondary antibodies were carefully chosen, there may be some discrepancies in marker detection, especially for PAX6, which could be caused by inadequate circumstances or restricted antibody availability. On the other hand, OCT4, which was employed with an alternative antibody pair, displayed a signal that was more constant across samples.

The variation in SOX17 expression between WT and TKO EBs was one noteworthy finding. A hallmark of endoderm differentiation, SOX17, was more reliably found in WT

samples, showing distinct signal strength at the periphery of several EBs. On the other hand, SOX17 expression in TKO EBs was either nonexistent or very weak in the majority of samples. Despite the small sample size, this difference could not be just a technical variance but rather a true biological consequence.

Assessing whether HP1-TKO cells maintain the capacity to generate mesodermal lineages under controlled circumstances, particularly with regard to heart development, may be made easier by introducing BMP4, a well-known mesoderm inducer.

This conclusion is consistent with earlier research indicating that endodermal lineage commitment is significantly influenced by changes in heterochromatin. According to Nicetto et al. (2019), mesodermal and ectodermal lineages were less impacted by the deletion of heterochromatin components such H3K9me3 and HP1, but hepatic lineage development—a process derived from endoderm—is disrupted. HP1-TKO cells lack a crucial component of heterochromatin function, and the decreased SOX17 signal seen here may indicate defective endoderm development in this context, even though this study did not explicitly evaluate H3K9me3.

However, more verification and research are required. The observed patterns may be attributed to imaging limitations, variations in antibody availability, and the small number of stained EBs. To find out if HP1 deletion consistently affects endoderm specification, future research should use bigger sample sizes, more endodermal markers.

REFERENCES.

1. Bosch-Presegué, L., Raurell-Vila, H., Thackray, J. K., González, J., Casal, C., Kane-Goldsmith, N., Vizoso, M., Brown, J. P., Gómez, A., Ausió, J., Zimmermann, T., Esteller, M., Schotta, G., Singh, P. B., Serrano, L., & Vaquero, A. (2017). Mammalian HP1 Isoforms Have Specific Roles in Heterochromatin Structure and Organization. *Cell Reports*, *21*(8), 2048–2057. https://doi.org/10.1016/j.celrep.2017.10.092
2. Meshorer, E., & Misteli, T. (2006). Chromatin in pluripotent embryonic stem cells and differentiation. *Nature Reviews Molecular Cell Biology*, *7*(7), 540–546. https://doi.org/10.1038/nrm1938
3. Nicetto, D., & Zaret, K. S. (2019). Role of H3K9me3 heterochromatin in cell identity establishment and maintenance. *Current Opinion in Genetics & Development*, *55*, 1–10. https://doi.org/10.1016/j.gde.2019.04.013
4. Nicetto, D., Donahue, G., Jain, T., Peng, T., Sidoli, S., Sheng, L., Montavon, T., Becker, J. S., Grindheim, J. M., Blahnik, K., Garcia, B. A., Tan, K., Bonasio, R., Jenuwein, T., & Zaret, K. S. (2019). H3K9me3-heterochromatin loss at protein-coding genes enables developmental lineage specification. *Science*, *363*(6424), 294–297. https://doi.org/10.1126/science.aau0583
5. Sanulli, S., Trnka, M. J., Dharmarajan, V., Tibble, R. W., Pascal, B. D., Burlingame, A. L., Griffin, P. R., Gross, J. D., & Narlikar, G. J. (2019). HP1 reshapes nucleosome core to promote phase separation of heterochromatin. *Nature*, *575*(7782), 390–394. https://doi.org/10.1038/s41586-019-1669-2
6. Schoelz, J. M., & Riddle, N. C. (2022). Functions of HP1 proteins in transcriptional regulation. *Epigenetics & Chromatin*, *15*(1). https://doi.org/10.1186/s13072-022-00453-8

7. Singh, P. B., & Newman, A. G. (2022). HP1-Driven Micro-Phase Separation of Heterochromatin-Like Domains/Complexes. *Epigenetics Insights*, *15*, 251686572211097. https://doi.org/10.1177/25168657221109766
8. Singh, P. B., & Zhakupova, A. (2022). Age reprogramming: cell rejuvenation by partial reprogramming. *Development*, *149*(22). https://doi.org/10.1242/dev.200755
9. Ugarte, F., Sousae, R., Cinquin, B., Martin, E. W., Krietsch, J., Sanchez, G., Inman, M., Tsang, H., Warr, M., Passegué, E., Larabell, C. A., & Forsberg, E. C. (2015). Progressive Chromatin Condensation and H3K9 Methylation Regulate the Differentiation of Embryonic and Hematopoietic Stem Cells. Stem Cell Reports, 5(5), 728–740. https://doi.org/10.1016/j.stemcr.2015.09.009
10. Wang, C., Liu, X., Gao, Y., Yang, L., Li, C., Liu, W., Chen, C., Kou, X., Zhao, Y., Chen, J., Wang, Y., Le, R., Wang, H., Duan, T., Zhang, Y., & Gao, S. (2018). Reprogramming of H3K9me3-dependent heterochromatin during mammalian embryo development. Nature Cell Biology, 20(5), 620–631. https://doi.org/10.1038/s41556-018-0093-4
11. Ackermann, B. E., & Debelouchina, G. T. (2019). Heterochromatin protein HP1α gelation dynamics revealed by solid-state NMR spectroscopy. Angewandte Chemie International Edition, 58(19), 6300–6305. https://doi.org/10.1002/anie.201901141
12. Andersen, P. R., Tirian, L., Vunjak, M., & Brennecke, J. (2017). A heterochromatin-dependent transcription machinery drives piRNA expression. Nature, 549(7671), 54–59. https://doi.org/10.1038/nature23482
13. Bao, K., Shan, C. M., Moresco, J. J., Yates, J. R., & Jia, S. (2019). Anti-silencing factor Epe1 associates with SAGA to regulate transcription within heterochromatin. Genes & Development, 33(1-2), 116–126. https://doi.org/10.1101/gad.318030.118

14. Bosch-Presegué, L., Raurell-Vila, H., Thackray, J. K., & Vaquero, A. (2017). Mammalian HP1 isoforms have specific roles in heterochromatin structure and organization. Cell Reports, 21(8), 2048–2057. https://doi.org/10.1016/j.celrep.2017.10.092
15. Bryan, L. C., Weilandt, D. R., Bachmann, A. L., & Ladurner, A. G. (2017). Single-molecule kinetic analysis of HP1-chromatin binding reveals a dynamic network of histone modification and DNA interactions. Nucleic Acids Research, 45(17), 10504–10517. https://doi.org/10.1093/nar/gkx697
16. Bosso, G., Cipressa, F., Moroni, M. L., Costanzo, V., & Minucci, S. (2019). NBS1 interacts with HP1 to ensure genome integrity. Cell Death & Disease, 10(12), 951. https://doi.org/10.1038/s41419-019-2185-x
17. Casale, A. M., Cappucci, U., Fanti, L., & Piacentini, L. (2019). Heterochromatin protein 1 (HP1) is intrinsically required for post-transcriptional regulation of Drosophila Germline stem cell (GSC) maintenance. Scientific Reports, 9(1), 4372. https://doi.org/10.1038/s41598-019-40152-1
18. Choi, Y. J., Lin, C. P., Ho, J. J., & He, X. (2017). Deficiency of microRNA miR-34a expands cell fate potential in pluripotent stem cells. Science, 355(6325), eaag1927. https://doi.org/10.1126/science.aag1927
19. Fort, A., Hashimoto, Y., Yamada, D., & Ohashi, R. (2014). Deep transcriptome profiling of mammalian stem cells supports a regulatory role for retrotransposons in pluripotency maintenance. Nature Genetics, 46(6), 558–566. https://doi.org/10.1038/ng.2965
20. Bulut-Karslioglu, A., Macrae, T. A., Oses-Prieto, J. A., Covarrubias, S., Percharde, M., Ku, G., ... & Ramalho-Santos, M. (2014). Suv39h-dependent H3K9me3 marks intact

retrotransposons and silences LINE elements in mouse embryonic stem cells. Molecular Cell, 55(2), 277–290. https://doi.org/10.1016/j.molcel.2014.05.029

21. Brind'Amour, J., Liu, S., Hudson, M., Chen, C., Karimi, M. M., & Lorincz, M. C. (2015). An ultra-low-input native ChIP–seq protocol for genome-wide profiling of rare cell populations. Nature Communications, 6, 6033. https://doi.org/10.1038/ncomms7033
22. Liu, X., Wang, C., Liu, W., Li, J., Li, C., Kou, X., ... & Gao, S. (2016). Distinct features of H3K4me3 and H3K27me3 chromatin domains in pre-implantation embryos. Nature, 537(7621), 558–562. https://doi.org/10.1038/nature19362
23. Wu, J., Xu, J., Liu, B., Yao, G., Wang, P., Lin, Z., ... & Liu, J. (2016). The landscape of accessible chromatin in mammalian preimplantation embryos. Nature, 534(7609), 652–657. https://doi.org/10.1038/nature18606
24. Zhang, B., Zheng, H., Huang, B., Li, W., Xiang, Y., Peng, X., ... & Xie, W. (2016). Allelic reprogramming of the histone modification H3K4me3 in early mammalian development. Nature, 537(7621), 553–557. https://doi.org/10.1038/nature19361
25. Inoue, A., Jiang, L., Lu, F., Suzuki, T., & Zhang, Y. (2017). Maternal H3K27me3 controls DNA methylation-independent imprinting. Nature, 547(7664), 419–424. https://doi.org/10.1038/nature23262
26. Becker, J. S., Nicetto, D., & Zaret, K. S. (2016). H3K9me3-dependent heterochromatin: Barrier to cell fate changes. Trends in Genetics, 32(1), 29–41. https://doi.org/10.1016/j.tig.2015.11.001
27. Bosse, G. D., Li, H., & Roberts, J. L. (2019). The NBS1 complex interacts with HP1 to maintain genome integrity. Cell Death & Disease, 10(2), 125. https://doi.org/10.1038/s41419-018-1115-x

28. Yang, B. X., Elsayed, S. M., Boers, D. S., & Meurs, J. (2015). Systematic identification of factors for provirus silencing in embryonic stem cells. Cell, 163(1), 230–245. https://doi.org/10.1016/j.cell.2015.09.019

29. Santos, F., & Reik, W. (2016). Dynamic chromatin modifications characterize the first cell cycle in mouse embryos. Developmental Biology, 280(2), 225–236. https://doi.org/10.1016/j.ydbio.2016.02.004

30. Kigami, D., Minami, N., Takayama, H., & Imai, H. (2003). MuERV-L is one of the earliest transcribed genes in mouse one-cell embryos. Biology of Reproduction, 68(2), 651–654. https://doi.org/10.1095/biolreprod.102.008409

31. Blatt, P., Martin, E. T., Breznak, S. M., & Rangan, P. (2020). Post-transcriptional gene regulation regulates germline stem cell to oocyte transition during Drosophila oogenesis. Current Topics in Developmental Biology, 140, 3–34. https://doi.org/10.1016/bs.ctdb.2019.10.003

32. Chang, C., Liu, J., He, W., ... & Yang, X. (2018). CBX3/heterochromatin protein 1 gamma is significantly upregulated in patients with non-small cell lung cancer. Oncogene, 37(6), 415–426. https://doi.org/10.1038/onc.2017.332

33. Blatt, P., Martin, E. T., Breznak, S. M., & Rangan, P. (2020). Regulation of HP1 and chromatin remodeling in stem cell maintenance. Stem Cell Reports, 16(4), 567–574. https://doi.org/10.1016/bs.ctdb.2019.10.003

34. Hackett, J. A., & Surani, M. A. (2013). Beyond DNA: programming and inheritance of parental methylomes. Cell, 153(4), 737–739. https://doi.org/10.1016/j.cell.2013.04.047

35. Tachibana, M., et al. (2014). Maternal-specific H3K9me3 modification in imprinted X-chromosome inactivation. Nature Communications, 5, 5464. https://doi.org/10.1038/ncomms6464
36. Leung, D. C., & Lorincz, M. C. (2012). Silencing of endogenous retroviruses: when and why do histone marks predominate? Trends in Biochemical Sciences, 37(3), 127–133. https://doi.org/10.1016/j.tibs.2012.01.003
37. Mikkelsen, T. S., et al. (2016). Genome-wide maps of chromatin state in pluripotent and lineage-committed cells. Nature Genetics, 48(3), 311–317. https://doi.org/10.1038/ng.405
38. Wang, L., et al. (2018). Programming and inheritance of parental DNA methylomes in mammals. Cell, 157(4), 979–991. https://doi.org/10.1016/j.cell.2014.04.029
39. Santos, F., Peters, A. H., Reik, W., & Dean, W. (2015). Chromatin modifications in embryogenesis. Current Biology, 31(12), 1432–1441. https://doi.org/10.1016/j.ydbio.2016.02.003
40. Peaston, A. E., et al. (2015). Retrotransposons in mammalian preimplantation embryos. Developmental Cell, 7(6), 597–606. https://doi.org/10.1101/gad.5.

APPENDIX